Computational insights into *Caenorhabditis elegans* vulval development

Jasmin Fisher*†, Nir Piterman*, E. Jane Albert Hubbard‡, Michael J. Stern§, and David Harel*

*Department of Computer Science and Applied Mathematics, Weizmann Institute of Science, Rehovot 76100, Israel; ‡Department of Biology, New York University, New York, NY 10003-6688; and §Department of Genetics, Yale University School of Medicine, New Haven, CT 06520-8005

Communicated by Richard M. Karp, International Computer Science Institute, Berkeley, CA, December 17, 2004 (received for review July 22, 2004)

Studies of *Caenorhabditis elegans* vulval development provide a paradigm for pattern formation during animal development. The fates of the six vulval precursor cells are specified by the combined action of an inductive signal that activates the EGF receptor mitogen-activated PK signaling pathway (specifying a primary fate) and a lateral signal mediated by LIN-12/Notch (specifying a secondary fate). Here we use methods devised for the engineering of complex reactive systems to model a biological system. We have chosen the visual formalism of statecharts and use it to formalize Sternberg and Horvitz's 1989 model [Sternberg, P. W. & Horvitz, H. R. (1989) *Cell* 58, 679–693], which forms the basis for our current understanding of the interaction between these two signaling pathways. The construction and execution of our model suggest that different levels of the inductive signal induce a temporally graded response of the EGF receptor mitogen-activated PK pathway and make explicit the importance of this temporal response. Our model also suggests the existence of an additional mechanism operating during lateral specification that prohibits neighboring vulval precursor cells from assuming the primary fate.

computational modeling | statecharts | LIN-12/Notch

The increasing usefulness of computational models in biology has led to the development of many different types of modeling approaches (1–3). The resemblance between reactive systems (computerized systems that interact continuously with their environment) and biological systems suggests the use of methods devised for the construction of complex reactive systems to model biological systems (4, 5). Such methods have already been used to model specific aspects of T cell activation (5) and differentiation in the thymus (6). This study is part of an ongoing project to model vulval development in *Caenorhabditis elegans* (7, 8).

These efforts have used two complementary approaches to model biological behavior: an intraobject approach based on the language of *statecharts* (ref. 9; *Supporting Materials*, which is published as supporting information on the PNAS web site) and the RHAPSODY tool (ref. 10; *Supporting Materials*) and an interobject approach that uses the language of *live sequence charts* (LSCs) (11) and the PLAY-ENGINE tool (12). Both statecharts and LSCs are visual languages that have a clear and rigorously defined syntax and semantics that enable the construction and execution of a formal model. Statecharts specify the full state-based behaviors of each object in the system (e.g., a cell), whereas LSCs specify the multimodal (e.g., allowed, forbidden, and necessary) scenarios that link together the objects by their sequences of behavior.

For clarity, we refer to the working models that biologists usually represent in their articles by annotated pictures as "diagrammatic models." These pictorial models themselves are static but are intended to be dynamically understood by the abstract reasoning of the reader. We contrast these with the kinds of "dynamic models" we construct, which are designed primarily for computerized execution and simulation by having formal support for their dynamic progression in time.

This article focuses on using statecharts to create a formal dynamic model of vulval fate specification based solely on the proposed diagrammatic model of Sternberg and Horvitz (13). The molecular and mechanistic aspects of vulval fate specification are currently understood at a much more detailed level than in 1989. Nonetheless, ref. 13 forms the basis for the current extended understanding of vulval fate specification by defining the relationships between two genetic mechanisms that underlie the cellular interactions involved in it. We stress that our dynamic model does not incorporate additional (newer) data than those in ref. 13.

The *C. elegans* vulva normally derives from three vulval precursor cells (VPCs) that are members of a larger set of six VPCs, P3.p–P8.p. Each of the six VPCs is multipotent, capable of adopting one of three fates, termed primary (1^0), secondary (2^0), or tertiary (3^0) (13–15). The actual fate that each cell adopts depends on intercellular signals: an inductive signal emanating from the gonadal anchor cell (AC), a lateral signal between VPCs, and an inhibitory signal from the surrounding hypodermal syncytium. Despite the ability of each cell to adopt any of the three fates, the pattern of fates adopted by P3.p–P8.p in wild-type animals is always $3^0\ 3^0\ 2^0\ 1^0\ 2^0\ 3^0$, respectively.¶ VPC fates in wild-type animals are influenced by their distance from the AC: the cell closest to the AC (P6.p) becomes 1^0, the next closest (P5.p and P7.p) become 2^0, and the most distant cells (P3.p, P4.p, and P8.p) become 3^0 (17–19).

Sternberg and Horvitz (13) described the fates of the VPCs in animals in which the inductive, inhibitory, and lateral signaling pathways were perturbed in various combinations and manners. Here, as in ref. 13, we refer collectively to mutations that interfere with the inductive signaling pathway (causing a vulvaless phenotype) as *Vul* and to *lin-15* mutations that interfere with the inhibitory pathway (causing a multivulva phenotype) as *Muv*. Lateral signaling can be affected by mutations in *lin-12*, a gene that encodes a *C. elegans* member of the Notch family of receptors. The *Vul* genes act in the EGF receptor mitogen-activated PK (EGFR-MAPK) inductive signaling pathway. The inductive signal is encoded by the *Vul* gene *lin-3* (20, 21). Here, as in ref. 13, we refer to this signal as the inductive signal, whereas (in accordance with ref. 13) we refer to the response to this signal within the VPCs as the "vulval signal." Although the *Muv* gene *lin-15* is currently considered part of the inhibitory pathway (22), it can be positioned in a genetic hierarchy so as to interfere with the vulval signal; mutation of *lin-15* results in activation of the vulval signal independent of the inductive signal. *lin-15* is treated in this manner in Sternberg and Horvitz (13), and we have dealt with it similarly here. In addition to reporting experimental data, Sternberg and Horvitz suggested a working model in diagrammatic form, supported by text, for interactions within and among VPCs during vulval induction (Fig. 1).

Abbreviations: VPC, vulval precursor cell; AC, anchor cell.

†To whom correspondence should be addressed. E-mail: jasmin.fisher@weizmann.ac.il.

¶In some animals, P3.p is not a member of the VPC equivalence group but instead fuses earlier with the hypodermal syncytium (16, 17).

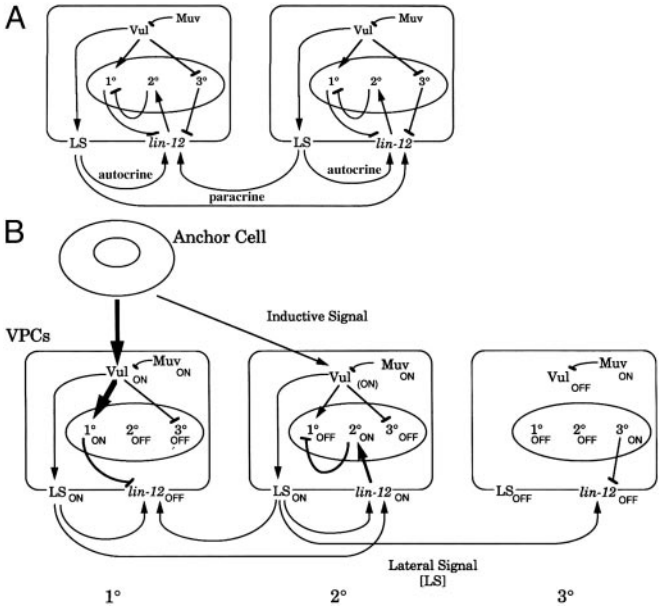

Fig. 1. Model for gene interactions during vulval induction. (*A*) Arrows represent activation, and bars represent inhibition. 1^0, 1^0-specific functions; 2^0, 2^0-specific functions; 3^0, 3^0-specific functions; LS, lateral signal. (*B*) ON, function is active; (ON), function is partially active; OFF, function is inactive. The thickness of each arrow indicates the strength of the interaction. [Reproduced with permission from ref. 13 (copyright 1989), with permission from Elsevier.]

We have formalized this diagrammatic model of Sternberg and Horvitz (13) as a dynamic computational model and report here on the ramifications of executing and analyzing this model by comparing it with the underlying data. Diagrammatic models in biology are often used to summarize a mechanistic understanding of a set of observations; in general, they represent a working hypothesis but do not make explicit features that are not sufficiently understood. To create a dynamic model that behaves in a manner consistent with the observed biological behavior, we have introduced several additional features that were not explicit in Sternberg and Horvitz's (13) diagrammatic model. The construction and analysis of the dynamic model has provided insights that aid our understanding of the VPC fate specification process.

Methods

Constructing the Statechart Model. Statechart models are constructed by defining the objects in the system, both tangible and nontangible, and representing all of their possible states and behaviors. Our model consists of the AC object (Fig. 2) and a class of VPC objects (Fig. 3). An additional object, called the Organizer, aids in the initialization of simulations (i.e., setting the initial conditions for a particular execution). All of the VPCs have the same statechart; that is, each runs its own version of the same program simultaneously, based on the signals and events it receives. All VPCs begin with identical conditions (as members of an equivalence group) but may receive different levels of inductive signal depending on the distance of the VPC from the AC (Fig. 6, which is published as supporting information on the PNAS web site). Below we describe the statecharts of the various objects, starting with that of the AC (Fig. 2).

The instantiation of the AC starts with the evaluation of a condition between two states (Fig. 2, circled C). If the simulation starts with ACablated, the AC enters the ablated state; otherwise (Fig. 2, [else]), it enters the Formed state. The > symbol indicates that there is an action specified as taking place upon

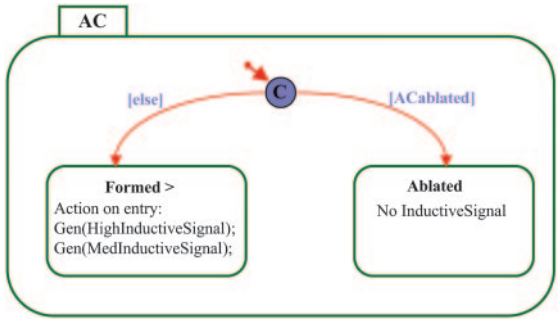

Fig. 2. The statechart of the AC. Rectangles represent states, and arrows represent transitions. A short arrow exiting a small circle marks the initial state of the object. The circled C denotes a condition between two states. A transition from a condition is taken if the guard is true.

entry to this state. This action evaluates the distance between the AC and each VPC and then sends a high inductive signal to the nearest VPC and a medium inductive signal to the next closest VPCs. Fig. 6 shows the Rhapsody form in which this has been specified.

The statechart of the VPC is more complex, because it contains five orthogonal components, separated by dashed lines (Fig. 3*A*). Orthogonal components are semiindependent portions of the behavior of an object. Describing the behavioral state of an object requires specifying the behavioral state of each of these components. In the case of the VPC in this model, these include a main component, representing the fate specification of the VPC, and components that represent the state of the *Vul*, *Muv*, and *lin-12* genes as well as of the Lateral Signal. We now describe each component briefly.

The Muv component captures the mutation status of *lin-15*, as mutated to an inactive state (MuvMutated) or not mutated (MuvNotMutated). It starts with a condition connector: if and when *lin-15* is specified as mutated, the VPC enters the MuvMutated state, and there is no *lin-15* activity and, hence, no inhibition of the vulval signal (No MuvInhibition). Alternatively, if *lin-15* is wild type, the VPC is in the MuvNotMutated state, and the action specified on entry to this state (note the > symbol) is to generate MuvInhibition.

The Vul component captures the status of the process carried out by the set of *vul* genes (i.e., *lin-2*, *lin-3*, *lin-7*, *lin-10*, and *let-23)*. Mutational inactivation of any one of these genes inactivates the Vul component.‖ This component also starts with a condition connector, so that if a Vul gene is specified as mutated, the VPC enters the VulMutated state and there is no Vul gene activity. If all Vul genes are wild type, the VPC enters the VulNotMutated state. The ellipsis appended to the VulNotMutated state name indicates the presence of a subchart, which is actually a zoom into this state. This subchart, which is shown in Fig. 3*B*, serves to integrate the MuvInhibition and the level of the InductiveSignal to determine the level of VulSignal pathway activity. MuvInhibition causes a transition to the Off state. According to Sternberg and Horvitz's diagrammatic model (13), *lin-15* constitutively inhibits the Vul pathway; thus, if MuvInhibition occurs, Vul pathway activity is in the Off state. The transition from Off to On takes place with the receipt of a high inductive signal (coming from the AC). When in the On state, the VPC generates a high vulval signal. Receipt of a medium inductive signal (from the AC) while in the Off state triggers a transition to the PartialOn state. This transition is accomplished in two steps. The VPC first enters the BeforePartialOn state for a period of 10 ms, and it then enters the PartialOn state. The time

‖The VulMutation condition can be thought of as a disjunction over these five genes.

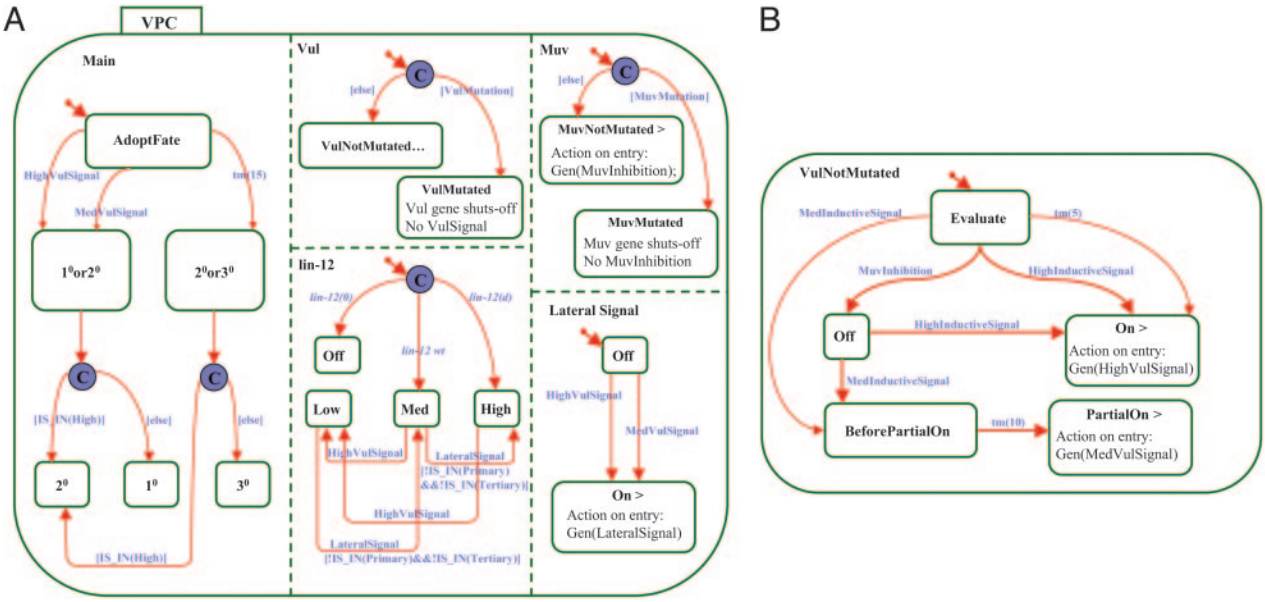

Fig. 3. The statechart of the VPC. (*A*) The high-level statechart of the VPC. Areas separated by dashed lines are orthogonal components; i.e., the VPC is present in all these components simultaneously. (*B*) The VulNotMutated substate. A zoom into the VulNotMutated state shows the various states and actions present within this state.

delay allows for the proper temporal integration of the lateral and inductive signaling pathways (see *The Kinetics of Competing Signaling Pathways*). When it is in the PartialOn state, the VPC generates a medium vulval signal. In the case that no MuvInhibition occurs and no inductive signal is received, after a period of 5 ms, a transition to the On state occurs. Note that the periods (5 or 10 ms) are not biologically accurate. They are a modeling means that we use to create a difference in the order of occurrence of the respective events.

The Lateral Signal component contains only Off and On states. The default is Off, whereas the transition to an On state depends on the VulSignal (high or medium). The action on entry to the On state is to send an autocrine and paracrine lateral signal. When it is in the On state, the VPC sends a LateralSignal (which is received by LIN-12) to itself and to its immediate neighbors.

The lin-12 component represents the level of *lin-12* activity and also starts with a condition. If *lin-12* activity is specified as wild type (*lin-12 wt*), its activity level is given as Medium. If *lin-12* activity is eliminated [*lin-12(0)* mutation], then the lin-12 component enters the Off state. By contrast, increasing *lin-12* activity [*lin-12(d)* mutation] leads to the High state. The transition from Med or High to Low occurs if a HighVulSignal is received. The transition from Low to Med is due to a lateral signal event, and this transition cannot occur when the VPC is about to assume a primary or tertiary fate (denoted by [!IS IN(Primary)&&!IS IN(Tertiary)]). The same guarding condition applies also to the transition from Med to High. It is important to note that, whereas some of the other arrows in Sternberg and Horvitz's model (13) were translated in our statechart into events, the arrow coming out of *lin-12* in the diagrammatic model (Fig. 1) was translated into three possible gene activity levels in the VPC statechart. Originally, we implemented the action of *lin-12* as an event, but to ensure that this event arrived exactly at the correct time, we had to incorporate more timing constraints into our model. Changing the lin-12 component to accommodate the *lin-12* activity level (Off, Low, Medium, or High), rather than modeling it as a direct event, circumvented this problem.

The Main component starts in the AdoptFate state. After a VulSignal (high or medium), the VPC enters the state "1^0 or 2^0." The reason for this intermediate state is explained below (see *Additional Control of Lateral Specification*). Emanating from this state is a condition specifying that if the *lin-12* level is High, the VPC becomes 2^0; otherwise, it becomes 1^0. However, if the system remains in the AdoptFate state for 15 ms and there is no VulSignal, the VPC enters state "2^0 or 3^0" (see *The Kinetics of Competing Signaling Pathways*), after which a condition specifies that if the *lin-12* level is High, the VPC becomes 2^0, and otherwise it becomes 3^0. Again, the duration of the 15-ms interval is arbitrary; it need only take longer than the 10-ms delay in the Vul component.

Testing the Statechart Model. After constructing the statechart model, we tested it in the following manner. First, we ran it under each of the general conditions corresponding to the experiments described in tables 1–3 of Sternberg and Horvitz (13).** Second, we compared the outcomes of the simulations with the actual observations as summarized in table 4 of Sternberg and Horvitz (13). Inconsistencies between the results from the computational model execution and the biological data reported in ref. 13 were used to reevaluate and adjust the computational model. This process was reiterated until the simulations reflected the actual observations described.

Results

Gaps Between the Dynamic Model and the Biological Observations. The iterative model-building strategy that we used highlighted the crucial role of two additional aspects of VPC fate specification: (*i*) the race between the pathways promoting 1^0 vs. 2^0 fate and (*ii*) the importance of additional control over lateral specification. We discuss these two aspects below.

The Kinetics of Competing Signaling Pathways. One of the main temporal issues that we had to take into account was the "race"

**The number of ACs was represented as present or absent, and VPC fates were categorized as 1^0, 2^0, or 3^0, not by specific lineages. The genetic conditions that were tested did not distinguish the individual genotypes but instead were represented as the class of mutation (*Muv*, *Vul*, and *lin-12*). These abstractions are similar to those used in Sternberg and Horvitz (13).

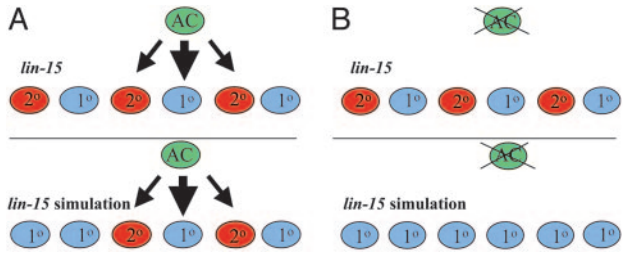

Fig. 4. Additional mechanism governing the lateral specification. Experimental results were compared with simulation results of *Muv* mutation in the presence (*A*) and absence (*B*) of AC.

between the two following sequences of events relevant to a given VPC:

(*i*) Inductive signal → vulval signal → primary fate.
(*ii*) Inductive signal received by neighbor → vulval signal in neighbor → lateral signal from neighbor → increased *lin-12* activity → secondary fate.

These two sequences of events need to be temporally prioritized, depending on the strength of the inductive signal received by an individual VPC and its neighboring VPCs. For example, the first of these sequences must proceed more rapidly than the second if a VPC exposed to the highest level of inductive signal is to acquire a 1^0 fate. Conversely, the second of these sequences must proceed more rapidly than the first if a VPC exposed to an intermediate level of inductive signal is to acquire a 2^0 fate. To effect this temporal prioritization, we had to introduce timing constraints into our dynamic computational model (Fig. 3*A*). Therefore, a mechanism was added by which a high inductive signal immediately induces a high vulval signal, whereas a medium inductive signal induces a medium vulval signal only after a time delay, arbitrarily set at 10 ms [the tm(10) arrow in Fig. 3*B*].

Additional Control of Lateral Specification. Representing the behavior of a *lin-15* mutant presented a second issue. The wild-type activity of *lin-15* normally constrains VPCs from adopting vulval fates unless they, or their neighbors, are exposed to the inductive signal (Movie 1, which is published as supporting information on the PNAS web site). Thus, in a *lin-15* mutant, all VPCs acquire one of the two vulval fates (1^0 or 2^0) independently of the inductive signal. Although an isolated VPC in a *lin-15* mutant background acquires a primary fate, it is well accepted that a *lin-12*-mediated mechanism, termed lateral specification, prohibits adjacent VPCs from both acquiring primary fates (23, 24). Here, we suggest that additional control is needed for the lateral specification to inhibit adjacent primary cells.

In our initial dynamic model, simulating the behavior of *lin-15* mutants created adjacent primary fates in certain circumstances in which biological observations showed this to occur very rarely. The underlying problem was traced to the fact that in our initial dynamic model [reflecting the 1989 diagrammatic model (13)], the VPCs advanced toward acquiring their fates simultaneously. Thus, despite having represented the *lin-12*-mediated lateral specification mechanism in the dynamic computational model, either all VPCs engaged this mechanism simultaneously and became secondary, or all VPCs did not engage this mechanism (simultaneously) and became primary (which is the behavior of the model depicted in Fig. 3).

Two examples of this discrepancy were observed. In the presence of the AC, the behavior predicted by the initial statechart-based simulation of a *lin-15* mutant was the cell fate pattern 1^0 1^0 2^0 1^0 2^0 1^0 (Fig. 4*A*). By contrast, the actual biological outcome is either 2^0 1^0 2^0 1^0 2^0 $1^0/2^0$ or 1^0 2^0 2^0 1^0 2^0 $1^0/2^0$. A second more blatant example was observed in the simulation of a *lin-15* mutant in which the AC had been ablated (Movie 2, which is published as supporting information on the PNAS web site). In this case, all VPCs were predicted by the model to become primary (Fig. 4*B*), whereas in the biological observations, adjacent primaries were extremely rare (13, 23). In this example, all of the VPCs became primary because they simultaneously reduced their ability to respond to the lateral signal and then sent lateral signals to their neighbors that were in turn ignored (simultaneously). The reason that P(5–7).p escape this simulation problem in the first example is that we had allocated a temporal priority to all VPC fates influenced by an inductive signal coming from the AC by delaying the response in VPCs that do not hear an inductive signal [the tm(5) arrow in Fig. 3*B*].

Therefore, we postulate that some additional mechanism is needed to allow different reactions to the lateral signal in neighboring VPCs. One possibility is to disallow the simultaneous progress of VPCs toward fate acquisition. For the simulations to fit the actual data for *lin-15* mutants, we added a special adjustment to our dynamic model to prohibit the simultaneous acquisition of vulval fates.

This simultaneity problem is reminiscent of a situation in computer science called "mutual exclusion," causing us to seek a computational solution based on the way the mutual exclusion problem is solved in computer science. Mutual exclusion refers to a situation in which a number of processes compete for access to a common commodity, often called the critical section. The solutions must guarantee that eventually all processes get the commodity, but that no two access it simultaneously. In our system, the ability to assume a 1^0 fate can be viewed as the critical section, with the additional constraint that no two adjacent VPCs have the ability to assume 1^0 fates simultaneously. It is important to note that all VPCs have the ability to assume a primary fate, even though, in most cases, not all of the VPCs in fact do so. Indeed, in the wild type, only one cell adopts this fate.

The situation that adjacent VPCs cannot simultaneously adopt primary fates is akin to a well known variant of the mutual exclusion problem, Dijkstra's "dining-philosophers" problem (25). This problem concerns six philosophers seated at a round table, alternating between phases of thinking and eating. Between every pair of neighboring philosophers, there is only a single fork (Fig. 7, which is published as supporting information on the PNAS web site). However, to eat, a philosopher has to acquire two forks, one to the right and one to the left of the place setting. The challenge is to devise a protocol for the philosophers to acquire, use, and release their forks in such a way that all of the philosophers eventually eat and none of them starves. A protocol to solve the dining-philosophers problem must satisfy the following requirements: mutual exclusion (no two philosophers use the same fork simultaneously) and freedom from deadlock and lockout (absence of starvation).

The dynamic model (as in Fig. 3) reproduces the erroneous behavior explained above. After a VPC enters state "1^0 or 2^0" or "2^0 or 3^0," the lateral signal is perceived (and in this case ignored), and then the VPC proceeds to evaluate the condition on *lin-12* level and assumes its fate. To address our own version of this problem and to make our computational model match the biological observations as closely as possible, we implemented a solution to the dining-philosophers problem that appears in the computer science literature. We added two subcharts to the intermediate states "1^0 or 2^0" and "2^0 or 3^0" in the Main component of the VPC statechart (Fig. 8, which is published as supporting information on the PNAS web site). With these subcharts in place, whenever a VPC is in the process of assuming a fate, its two neighbors have to wait until it finishes deciding what fate it adopts. When that happens, the lateral signal of the cell takes effect on its neighbors and they, in turn, assume a

different fate (secondary when *lin-12* is present). Thus, neighboring VPCs cannot assume vulval fates simultaneously, but all VPCs have the ability to assume a vulval fate eventually. This allowed all initial conditions to result in simulations that matched the biological results (Movie 3, which is published as supporting information on the PNAS web site), suggesting that nonsimultaneous fate acquisition allows the lateral specification mechanism to take effect.

A final comment is necessary concerning the ability of our model to represent the biological variability of fates in nonnormal situations. Although the simulations that we obtained with our dynamic model are consistent with the biological results, the fact that the model is completely deterministic prevents it from being able to reproduce the fate variability observed biologically. Thus, for example, whereas P8.p can acquire either a primary or secondary fate in a *lin-15* mutant (23), the simulated behavior using this model always generates a primary fate for P8.p. Extended versions of this model will incorporate nondeterminism to represent the biological variability more accurately.

Discussion

We have constructed and tested a computerized dynamic model representing key aspects of VPC fate specification in *C. elegans*. This was done by translating the static, diagrammatic model from the landmark paper of Sternberg and Horvitz (13) into a dynamic model using the language of statecharts. The way in which this was done provides the basis for incorporating additional knowledge concerning VPC specification into extensions of the model. Since 1989, our understanding of vulval fate specification has become quite sophisticated and complex. As such developmental phenomena become understood in increasingly greater detail, the influence of time on system behavior becomes an increasingly important, if experimentally daunting, component to incorporate.

Describing working models in a formal language, especially one that is dynamic and executable by computer, has distinct advantages in the necessary incorporation of a time component in describing biological behaviors. First, a formal language comes with a rigorous semantics that goes beyond the simple positive and negative interaction symbols typically used in diagrammatic working models. Second, formal dynamic models can represent phenomena of importance to biology that static models cannot represent, such as time, concurrency, and simultaneity. If the language used to formalize the model is intended for describing dynamic processes, the semantics, by its very nature, provides the means for tracing the dynamics of system behavior, which is really the ability to run, or execute, the models described therein. Third, when a formal model is executable, the modeler must provide all parts of the model that are crucial for its execution.

This last aspect of formal modeling may appear as a hindrance to biologists, because there are many mechanistic "gaps" in our understanding of most biological processes. Nonetheless, by requiring those parts of the model that are crucial for its execution (hypothetical or not), the modeling process is itself useful in two ways. First, gaps that are logical in nature (that is, mechanisms that are not included in the static model but are intended to be provided, consciously or subconsciously, by abstract reasoning) are relatively easy to discover. By highlighting these deficits, modeling efforts can stimulate new hypotheses to test biologically. Often, such hypotheses can even be tested *in silico* before being tested experimentally. Second, the comparison of formal computational simulations with the same biological data used to construct the static diagrammatic model ensures that all experimental results are consistent with the original model proposed. In our case, when the statechart model was in place (based on the diagrammatic model), we were able to specify the experimental conditions as inputs, run the model, and then check the output of the run against the outcome of the actual experiments.

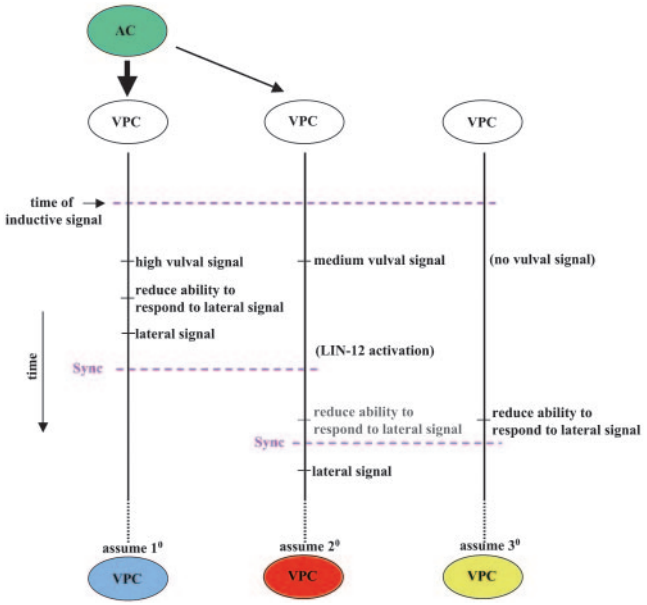

Fig. 5. Timing of events that occur in response to the different levels of inductive signal. This sequence diagram specifies a proposed order of events leading to VPC fate specification. Time flows from top to bottom. Two events on the same vertical line are ordered according to the time flow. The horizontal dashed lines synchronize the different vertical lines. All events above a synchronization line occur before an event below the synchronization line. The time order between two events on parallel vertical lines without a synchronization line is unknown. The drawing is not to scale; i.e., a longer distance between two events does not necessarily mean that the time elapsed between them is longer. The left time line starts with a high inductive signal, the middle time line starts with a medium inductive signal, and the right time line starts with no inductive signal. Events shown in black represent wild-type behavior. The event shown in gray ("reduce ability to respond to lateral signal") would occur in an isolated VPC (i.e., if the lateral signal is not received and does not trigger LIN-12 activation). In the abstraction level used, an event occurs when the system reaches a threshold that triggers an effective response.

By creating the dynamic computational model described here, we identified gaps and observed inconsistencies in the 1989 diagrammatic model (13). These gaps highlight important aspects of the biology of VPC fate specification that could lead to new experimental avenues to explore. New data could then be used to refine the model in a way that eliminates these gaps. The issues all revolve around time/synchronicity processes: the timing of signal transduction and reception and creating a difference between fate decisions of initially equivalent cells. To create a functional computational model that can simulate the known biological data, we implemented solutions to each of these issues, one of which is based on similarities with well known issues arising in computer science.

Our dynamic model explicitly requires that the responses to the inductive signal are graded not only spatially but also temporally. Specifically, we suggest that the time that it takes a high inductive signal to induce a lateral signal is less than the time that it takes a medium inductive signal to decrease the *lin-12* activity level. In addition, we postulate that, in reality, it takes less time to respond to a high than to a medium inductive signal, and this is the way our model is built. Our model is also set up so that the time that it takes to reduce *lin-12* activity in the absence of an inductive signal (which in our dynamic model signifies reduced ability to respond to the lateral signal) is less than the time that it takes a medium inductive signal to induce

the lateral signaling. This prevents VPCs that receive a medium signal but subsequently acquire a 2^0 fate from inducing a 2^0 fate in their AC-distal neighboring VPCs.

Based on these two time-ordering constraints, we generated a sequence diagram (Fig. 5) describing the ordering (over time) of the events that we incorporated into our dynamic model to regulate VPC fate acquisition. This represents our suggestion for how the system may work, reflecting our computational solution. The time order of events is linked to the level of the inductive signal received by a VPC. The inductive signal induces a vulval signal, which in turn induces a reduction in the ability to respond to the lateral signaling [decrease in *lin-12* level (26)], followed by lateral signaling and fate acquisition (in that order). In a VPC that does not receive an inductive signal, there is a reduction in the ability to respond to the lateral signaling, followed by 3^0 fate acquisition. We find that these are the minimal requirements that make our computational model consistent with the actual data. Changing any of these constraints impairs our ability to mimic *in silico* the actual behavior of the VPC fate-specification system.

As discussed earlier, *lin-15* mutants require an additional mechanism governing the lateral specification that prohibits neighboring VPCs from assuming the primary fate. Without such a mechanism, and in the absence of the AC, all VPCs would adopt a primary fate. If we assume that all VPCs have the same "blueprint," then either there is some external mechanism that prohibits them from advancing in exactly the same way and assuming primary fates, or there is some internal mechanism that forces them to assume different fates. Implementing an external mechanism that prohibits the cells from assuming fates simultaneously shows *in silico* that such a mechanism would indeed result in the desired phenotype.

Because the diagrammatic model was postulated in 1989 (13), explicit cellular and molecular mechanisms have begun to be elucidated that underlie some of the issues predicted by the diagrammatic model and highlighted by our formulation of the dynamic model. One example is the recent molecular identification of the lateral signal(s), which appears to consist of redundant soluble and membrane-bound ligands (27). A mechanism by which LIN-12 levels are reduced in response to induction [high vulval signal, in Sternberg and Horvitz's model (13)] has also been recently elucidated and shown to occur by the degradation of the LIN-12 protein (26). Putative targets of LIN-12-mediated signaling have recently been identified. These include a host of genes [*ark-1*, *lip-1*, *lst-1–4*, and *dpy-23* (28–30)] whose products interfere with the EGF receptor mitogen-activated PK (EGFR-MAPK) signaling pathway, helping to integrate these signaling pathways. Elucidation of the competition between the EGFR-MAPK signaling pathway and the lateral signaling pathway (28) has led Sternberg to suggest that the EGFR-MAPK signaling pathway should take long enough for the lateral signaling pathway to intercept it (31). Last, the time delay introduced between the 1^0 vs. 2^0 fate decision ("1^0 or 2^0" state) and the 2^0 vs. 3^0 decision ("2^0 or 3^0" state) is consistent with Ambros' work (32) on cell cycle-dependent sequencing of VPC cell fate decisions and subsequent work (33). Having established the core of a dynamic computational model for VPC fate specification, it is now possible to extend this model to incorporate the many biological features that have greatly enhanced our understanding of this system.

This work represents a step toward modeling that more sophisticated understanding of VPC fate specification. A state-based mechanistic model is particularly well suited for capturing the level of understanding obtained using the tools and approaches common in the field of developmental genetics. Nonetheless, other means for representing continuous phenomena can be incorporated into object-oriented models that employ languages like statecharts, resulting in hybrid models. Our statechart model also has the potential of interacting with the developing live sequence chart model of VPC specification (7) to take advantage of the complementary strengths of these two related representations.

Executing the computational model allowed an investigation of two time-dynamic processes: signal reception/triggered events and subsequent fate decisions among initially equivalent cells. Just as building the kinds of diagrammatic models used in developmental genetics helps to clarify mechanistic interactions and generate hypotheses to focus future research efforts, formalizing these models into statecharts is an intuitive way to add temporal dynamics into the model, thereby enhancing our understanding of biology. We propose that formal models of biological processes based on the tools developed for complex reactive systems offer an especially effective tool for exploring time-dependent processes in biological systems.

We thank S. Efroni and H. Kugler for generous help and advice in the initial phase of this project and N. Kam for initiating this line of research. This work was supported in part by the Minerva Foundation, National Institutes of Health Grants F5490-01 (to D.H.) and R24-GM066969 (to E.J.A.H., M.J.S., and D.H.), and Israel Science Foundation Grant 287/02 (to D.H.). N.P. was supported by the Minerva Foundation, and J.F. was supported by the Dov Biegun Postdoctoral Fellowship.

1. Bolouri, H. & Davidson, E. H. (2003) *Proc. Natl. Acad. Sci. USA* **100,** 9371–9376.
2. Ghosh, R., Tiwari, A. & Tomlin, C. (2003) in *Hybrid Systems: Computation and Control, Lecture Notes in Computer Science* (Springer, Berlin), Vol. 2623, pp. 233–248.
3. Raya, A., Kawakami, Y., Rodriguez-Esteban, C., Ibanes, M., Rasskin-Gutman, D., Rodriguez-Leon, J., Buscher, D., Feijo, J. A. & Izpisua Belmonte, J. C. (2004) *Nature* **427,** 121–128.
4. Harel, D. (2002) *Bull. Eur. Assoc. Theor. Comput. Sci.* **81,** 226–235.
5. Kam, N., Harel, D. & Cohen, I. R. (2001) in *Visual Languages and Formal Methods* (IEEE, Washington, DC), pp. 15–22.
6. Efroni, S., Harel, D. & Cohen, I. R. (2003) *Genome Res.* **13,** 2485–2497.
7. Kam, N., Harel, D., Kugler, H., Marelly, R., Pnueli, A., Hubbard, E. J. A. & Stern, M. J. (2003) in *Computational Methods in Systems Biology, Lecture Notes in Computer Science* (Springer, Berlin), Vol. 2602, pp. 4–20.
8. Fisher, J., Harel, D., Hubbard, J., Piterman, N., Stern, M. & Swerdlin, N. (2004) in *Computational Methods in Systems Biology, Lecture Notes in Computer Science* (Springer, Berlin), Vol. 3082.
9. Harel, D. (1987) *Sci. Comput. Program.* **8,** 231–274.
10. Harel, D. & Gery, E. (1997) *Computer* **30,** 31–42.
11. Damm, W. & Harel, D. (2001) *Formal Methods Syst. Des.* **19,** 45–80.
12. Harel, D. & Marelly, R. (2003) *Come, Let's Play: Scenario-Based Programming Using LSCs and the Play-Engine* (Springer, Berlin).
13. Sternberg, P. W. & Horvitz, H. R. (1989) *Cell* **58,** 679–693.
14. Sulston, J. E. & White, J. G. (1980) *Dev. Biol.* **78,** 577–597.
15. Sternberg, P. W. & Horvitz, H. R. (1986) *Cell* **44,** 761–772.
16. Sulston, J. E. & Horvitz, H. R. (1977) *Dev. Biol.* **56,** 110–156.
17. Chen, Z. & Han, M. (2000) *BioEssays* **22,** 503–506.
18. Kimble, J. (1981) *Dev. Biol.* **87,** 286–300.
19. Thomas, J. H., Stern, M. J. & Horvitz, H. R. (1990) *Cell* **62,** 1041–1052.
20. Katz, W. S., Hill, R. J., Clandinin, T. R. & Sternberg, P. W. (1995) *Cell* **82,** 297–307.
21. Hill, R. J. & Sternberg, P. W. (1992) *Nature* **358,** 470–476.
22. Herman, R. K. & Hedgecock, E. M. (1990) *Nature* **348,** 169–171.
23. Sternberg, P. W. (1988) *Nature* **335,** 551–554.
24. Greenwald, I. S., Sternberg, P. W. & Horvitz, H. R. (1983) *Cell* **34,** 435–444.
25. Dijkstra, E. W. (1971) *Acta Inf.* **1,** 115–138.
26. Shaye, D. D. & Greenwald, I. (2002) *Nature* **420,** 686–690.
27. Chen, N. & Greenwald, I. (2004) *Dev. Cell* **6,** 183–192.
28. Yoo, A. S., Bais, C. & Greenwald, I. (2004) *Science* **303,** 663–666.
29. Hopper, N. A., Lee, J. & Sternberg, P. W. (2000) *Mol. Cell* **6,** 65–75.
30. Berset, T., Hoier, E. F., Battu, G., Canevascini, S. & Hajnal, A. (2001) *Science* **291,** 1055–1058.
31. Sternberg, P. W. (2004) *Science* **303,** 637–638.
32. Ambros, V. (1999) *Development (Cambridge, U.K.)* **126,** 1947–1956.
33. Wang, M. & Sternberg, P. W. (1999) *Dev. Biol.* **212,** 12–24.